Cement & Concrete Composites 31 (2009) 693–698

Contents lists available at ScienceDirect

Cement & Concrete Composites

journal homepage: www.elsevier.com/locate/cemconcomp

Influential depth of moisture transport in concrete subject to drying–wetting cycles

Kefei Li *, Chunqiu Li, Zhaoyuan Chen

Civil Engineering Department, Tsinghua University, 100084 Beijing, PR China

ARTICLE INFO

Article history:
Received 3 September 2007
Received in revised form 28 August 2009
Accepted 28 August 2009
Available online 4 September 2009

Keywords:
Concrete
Drying–wetting cycles
Moisture transport
Durability
Influential depth

ABSTRACT

An analytical approach is used to investigate the influential depth over which moisture transport occurs within initially saturated concrete subjected to drying–wetting cycles. During drying the moisture transport is modelled as an evaporation–diffusion process with instantaneous evaporation at the moving gas–liquid interface, while the wetting of dried concrete surface zone is described by capillary absorption. Based on the water loss and intake balance during drying and wetting, an equilibrium drying–wetting time ratio is identified. By this ratio, the drying–wetting cycles are classified as drying-dominated, wetting-dominated and equilibrium ones. The corresponding moisture influential depths are expressed explicitly in terms of environmental factors and material transport properties. With the available concrete sorptivity data, the equilibrium time ratio and influential depth are calculated and discussed in depth.

1. Introduction

The deterioration of concrete structures by environmental actions has become a general concern for engineering design, maintenance and management [1]. Moisture (water) can either be a transport medium of external aggressive agents, e.g. CO_2 and chloride ions, or be itself a reactant of a degradation process, e.g. alkali–silica reaction. Accordingly most durability problems of structural concrete are intimately related to moisture transport. As concrete surface is exposed to drying–wetting cycles, the capillary absorption mechanism is mobilized so that the moisture transport and the ingression of external agents can be more efficient. The drying–wetting cycles are identified as the most unfavorable environmental condition for concrete deterioration processes [2,3]. Concrete is a porous material of low permeability with saturated permeability coefficients in the range of 10^{-14}–10^{-12} m/s [4]. For typical natural drying and wetting duration, the moisture loss and intake usually affect a rather limited depth from the concrete surface [5,6]. This depth is commonly noted as the influential depth of moisture transport.

The influential depth, and its dependencies on material design and environmental factors, has both scientific and practical significance. For laboratory research, this depth can help to set up rational drying–wetting schemes for accelerated durability tests and to investigate aggressive agent transport under drying–wetting cycles. For durability design of concrete structures, this depth can indicate directly the expected quality and thickness of concrete cover to steel reinforcement. The influential depth has been investigated by several authors: a unified diffusion model is used to calculate the humidity profile with constant moisture diffusivity [7]; saturation-dependent moisture diffusivity is taken into account by Arfvidsson [8] through an updated numerical scheme and by Cunningham [9] through an analytical approach; a lumped model is employed to investigate the effective transport depth of moisture for one-sided and two-sided cases under periodical moisture content with a constant diffusion coefficient [10].

However, most available approaches are limited in their abilities to predict moisture transport under natural drying–wetting cycles for the following reasons. (1) Different moisture transport mechanisms are mobilized during drying and wetting: during drying moisture migrates to the surface by a combined evaporation–diffusion–convection process while during wetting moisture transport is dominated by capillary absorption of liquid water [11,12]. So the water diffusivity function can not be the same for drying and wetting. (2) Relevant research shows the wetting of a porous material of low permeability by liquid water creates a sharp wetting front in the material [13,14], which is also plausible for the drying of a wet porous material. Thus, diffusion models giving a transitional humidity profile are no longer valid for moisture transport with drying and wetting fronts. (3) Under natural climates, wetting is closely related to liquid water accumulation on concrete surface by atmospheric precipitation or sea tide splashing, so natural cycles can have very different drying and wetting durations. The equal duration assumption retained in previous research for drying and wetting is not realistic.

Motivated by the dearth of satisfactory results on influential depth, this paper aims to investigate fundamental relationships

* Corresponding author. Tel./fax: +86 10 6279 7422.
E-mail address: likefei@tsinghua.edu.cn (K. Li).

0958-9465/$ - see front matter © 2009 Elsevier Ltd. All rights reserved.
doi:10.1016/j.cemconcomp.2009.08.006

amongst the influential depth, material transport properties and drying–wetting cycles. The paper is organized in the following way. In Section 2, the authors describe the drying and wetting of concrete by an evaporation–diffusion model and capillary absorption process, respectively, and the relevant mathematical equations are given. The concept of equilibrium time ratio for drying–wetting is proposed and the analytical expression of time ratio is derived in Section 3. By the established concept of time ratio, the influential depth of moisture transport is analyzed for different cases of drying–wetting time ratios and some numerical calculations are performed in Section 4. Concluding remarks are given in Section 5 for the developed concepts of time ratio and influential depth, as well as their application to structural case analysis.

2. Moisture transport

2.1. Evaporation–diffusion process for drying

For the sake of simplicity, an initially saturated state is considered for concrete during drying. As the concrete surface is exposed to a lower humidity during drying, the evaporation process occurs at the gas–liquid interface within the pore structure of concrete. Meanwhile, the evaporation elevates the local vapor concentration near the interface, which induces a vapor diffusion process from the interface to the concrete surface. The moisture transport during drying is modelled herein as such an evaporation–diffusion process.

Consider a one dimensional evaporation–diffusion process. At $t = 0$, the porous material is saturated by liquid water; at $t > 0$, the material is exposed to a lower humidity $h_0 < 100\%$ at the position $x = 0$. During the drying process, the gas phases in material pores are composed of dry air and vapor. The mass conservation of vapor can be expressed as,

$$\frac{\partial c_v}{\partial t} = \mathrm{div}(D_v \mathrm{grad} c_v) \tag{1}$$

where c_v stands for the molar concentration of vapor ($\mathrm{mol/m^3}$) in gas phases and D_v for vapor diffusion coefficient in concrete pore structure ($\mathrm{m^2/s}$). The vapor concentration c_v can be converted to its partial pressure p_v in gas phases by Claperon's equation and furthermore to relative humidity h by the standard definition of relative humidity,

$$p_v = RTc_v, \quad h = \frac{p_v}{p_{vs}} \tag{2}$$

with R as the perfect gas constant (J/mol/K), T the absolute temperature (K) and p_{vs} the saturated vapor pressure (Pa). Thus, Eq. (1) can be written in terms of relative humidity h,

$$\frac{\partial h}{\partial t} = \mathrm{div}(D_v \ \mathrm{grad} \ h) \tag{3}$$

Near the gas–liquid interface, the evaporation increases local vapor concentration, which will in turn elevate the local liquid water content in pores by condensation. If this condensation is considered as a local one, the vapor diffusion coefficient can be assumed constant between material surface $x = 0$ and the evaporation interface $x = X$. The boundary conditions are expressed in term of relative humidity,

$$\begin{cases} h(x = X, t) = h_s = 100\% \\ h(x = 0, t > 0) = h_0 < 100\% \end{cases} \tag{4}$$

At the gas–liquid interface $x = X$, the vapor molecules escape from gas–liquid interface by evaporation and transport to $x = 0$ by diffusion in dry air. As a first approximation, the evaporation rate is assumed to be much greater than the subsequent diffusion rate so that evaporation can be considered as instantaneous. The moisture mass conservation across the interface can thus be expressed as,

$$\rho_l \left(\frac{dX}{dt}\right) = M_v D_v \left(\frac{\partial c_v}{\partial x}\right)_{x=X} \tag{5}$$

with ρ_l representing the liquid water mass density ($\mathrm{kg/m^3}$) and M_v the vapor molar mass (kg/mol). Adopting the notation of relative humidity in Eq. (2), the above equation can be rewritten as,

$$\rho_l \left(\frac{dX}{dt}\right) = p_{vs} \frac{M_v}{RT} D_v \left(\frac{\partial h}{\partial x}\right)_{x=X} \tag{6}$$

Accordingly the moisture transport process is described by Eqs. (3), (4) and (6) which constitute a Stefan-like moving boundary problem. The solution procedure is detailed in Appendix A and the drying front position X is,

$$X = 2\lambda\sqrt{D_v t} \tag{7}$$

The drying front coefficient λ is the solution of the following equation,

$$\lambda \mathrm{erf}(\lambda) \exp(\lambda^2) = \frac{1}{\sqrt{\pi}} \frac{p_{vs}}{\rho_l} \frac{M_v}{RT} (h_s - h_0) \tag{8}$$

with erf(z) as error function. The humidity profile is,

$$h - h_0 = \frac{h_s - h_0}{\mathrm{erf}(\lambda)} \mathrm{erf}\left(\frac{x}{2\sqrt{D_v t}}\right) \quad 0 \leqslant x \leqslant X \tag{9}$$

2.2. Capillary absorption process for wetting

Consider a concrete initially unsaturated. As the material is put into contact with liquid water, the water intake is dominated by capillary absorption (suction) across the material surface. The available experimental results indicate, in a more detailed way, that the water intake is accomplished by an initial instantaneous surface sorption, a subsequent capillary sorption and a latent water diffusion at smaller (gel) pore level [11,12]. However, for the sake of simplicity a conceptual model of capillary transport is retained,

$$I_w = S_w\sqrt{t} \tag{10}$$

with I_w for water intake flow (m) and S_w for concrete sorptivity ($\mathrm{mm/min^{1/2}}$). The sorptivity depends on the water saturation degree in concrete s_l and can be expressed, according to Hall [13], as,

$$S_w = S_w^0(1 - 1.08s_l)^{\frac{1}{2}} \tag{11}$$

with S_w^0 for sorptivity measured from a totally dry sample.

3. Equilibrium drying–wetting time ratio

3.1. Concept of equilibrium time ratio

Now consider concrete surface subject to periodical drying–wetting cycles with a drying duration t_d and a wetting duration t_w for each cycle. Here we analyze the water loss and water intake for the first drying–wetting cycle. For the drying phase, the water loss flow I_d from a saturated state can be evaluated by the progression of drying front $X = X(t)$,

$$I_d = (s_s - s_0)X \tag{12}$$

with s_s, s_0 standing for the water saturation degree of concrete at the humidity levels of h_s and h_0, respectively. Here it is assumed that the elevation of water saturation near the drying front due to condensation is very local and the liquid water saturation between [0,X] is constant, equal to s_0. During the subsequent wetting phase, the water intake flow can be evaluated by Eqs. (10) and (11).

After the first drying–wetting cycle, if the water loss during drying and water intake during wetting reach an equilibrium state, $I_d = I_w$, one can assume that the drying zone [0,X] created in drying phase t_d is totally refilled in the subsequent wetting phase t_w. In other words, the drying front X is stabilized. By Eqs. (10)–(12) the above equilibrium condition can be written as,

$$I_d = I_w : \quad (s_s - s_0)X(t_d) = S_w\sqrt{t_w} \tag{13}$$

Substitution of Eq. (7) into the above equation gives,

$$(s_s - s_0)2\lambda\sqrt{D_v t_d} = S_w\sqrt{t_w} \tag{14}$$

An equilibrium time ratio τ_s, resulted from the equilibrium between water intake and water loss, is thus defined as,

$$\tau_s = \frac{t_d}{t_w} = \left[\frac{S_w}{2\lambda\sqrt{D_v}(s_s - s_0)}\right]^2 \tag{15}$$

3.2. Numerical analysis

To evaluate quantitatively the equilibrium time ratio τ_s, one has to detail the drying front coefficient λ and vapor diffusion coefficient D_v. By Eq. (8) the coefficient λ depends on the saturated vapor pressure p_{vs} and drying humidity gradient $\Delta h = h_s - h_0$. The vapor pressure p_{vs} is a function of ambient temperature T. Here we retain a regression function given by Mainguy [15],

$$p_{vs}(T) = \exp\left(68.18 - \frac{7214.64}{T} - 6.2973\ln T\right) \tag{16}$$

The diffusion coefficient D_v of vapor in concrete depends on the intrinsic diffusion coefficient of vapor in dry air D_{va} and the resistance of pore structure represented by a tortuosity function f,

$$D_v = D_{va}f \tag{17}$$

with D_{va} and f specified, respectively, in [16,17],

$$D_{va}(p_g, T) = 0.217\,\frac{p_{atm}}{p_g}\left(\frac{T}{T_0}\right)^{1.88}, \quad f = \phi^{4/3}(1 - s_l)^{10/3} \tag{18}$$

with D_{va} for vapor diffusion coefficient (cm^2/s), T for temperature (K), p_{atm} for atmospheric pressure (Pa), p_g for total pressure of dry air and vapor (Pa), ϕ for concrete porosity (–). It is assumed here that pore gas pressure is in permanent equilibrium with atmospheric pressure $p_g = p_{atm}$, and D_{va} depends only on temperature T. By Eqs. (11), (16), (17) and (18) the time ratio τ_s can be expressed in terms of variables S_0, s_l, T, ϕ,

$$\tau_s(S_0, s_l, T, \phi) = \left[\frac{S_w(S_0, s_l)}{2\lambda(T, h_s - h_0)\sqrt{D_v(T, \phi, s_l)}(s_s - s_0)}\right]^2 \tag{19}$$

It is to note that $h_s - h_0$ and $s_s - s_0$ are interdependent through concrete sorption isotherm function $h - s_l$, which can be derived from Kelvin equation and capillary pressure function $p_c(s_l)$. Adopting the capillary function from Mainguy [15], the sorption isotherm can be expressed as,

$$\rho_l\frac{RT}{M_v}\ln(h) = -p_c(s_l) = -a(s_l^{-b} - 1)^{1-\frac{1}{b}} \tag{20}$$

where a, b are experimental constants. This sorption isotherm is the very transport identity for concrete porous materials and includes more detailed moisture transport behaviours, such as the influence of salt presence [18].

With p_{vs} described in Eq. (16) a numerical scheme is developed to solve λ in Eq. (8). With the parameters retained in Table 1, the evolution of λ in terms of ambient temperature $\theta = T - 273$ and humidity gradient $\Delta h = h_s - h_0$ is illustrated in two dimensions and three dimensions, respectively, by Fig. 1a and b. It can be seen that for typical environmental temperature, $\theta = 0$–40 °C, the magnitude of λ is in the order of 10^{-3} and λ increases monotonically with ambient temperature and humidity gradient.

Table 1
Parameters for evaluation of equilibrium time ratio τ_s of drying–wetting cycles.

Parameters	Value
Perfect gas constant R (J/K/mol)	8.3147
Temperature T (K)	293.15
Saturated vapor pressure p_{vs} at 20 °C (kPa)	2.337
Atmospheric pressure p_{atm} (kPa)	101.325
Water density at 20 °C ρ_l (kg/m^3)	1000
Molar mass of vapor M_v (kg/mol)	0.018
Concrete internal humidity h_s (%)	100
Environmental humidity for drying h_0 (%)	20–90
Capillary pressure coefficient a (MPa) [15]	18.624
Capillary pressure coefficient b (–) [15]	2.275

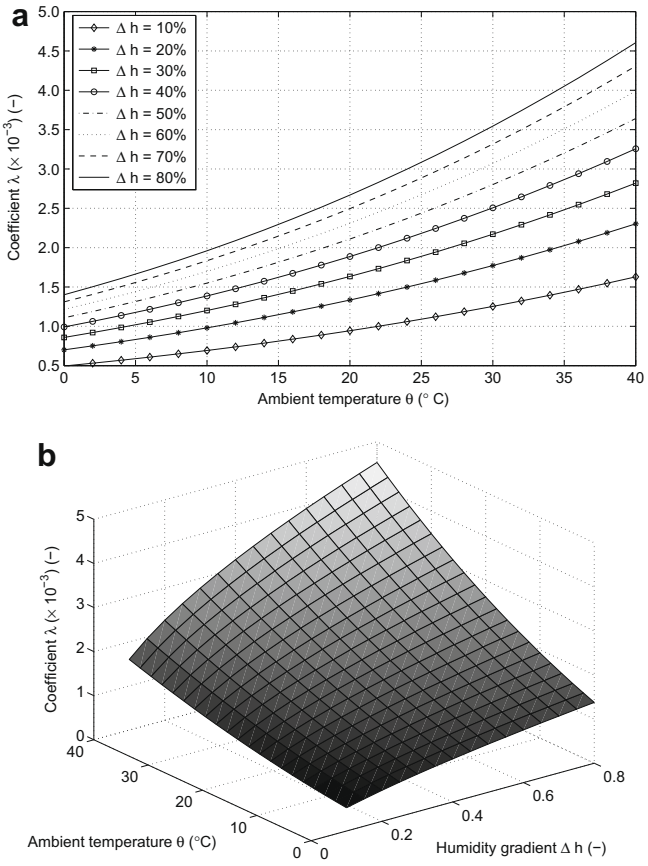

Fig. 1. Influential depth coefficient λ in terms of ambient temperature θ and external drying humidity gradient Δh. (a) Two dimensional illustration and (b) three dimensional illustration.

For the equilibrium time ratio expressed in Eq. (19), no attempt is undertaken to investigate the influence of all variables. Instead, five representative concrete samples from Hall [13] are retained with measured porosity and sorptivity at dry state (ϕ, S_0), and the time ratio τ_s is calculated in terms of humidity gradient Δh for an isothermal process at T = 293 K. The parameters for this calculation are given in Table 1 and the results are illustrated in Fig. 2a and b. For an easier interpretation of results, three horizontal lines are added on Fig. 2b, representing, respectively, time ratio τ_s of 50:1, 100:1 and 500:1. If the drying–wetting alternative period is taken as 1 year, in other words, the drying–wetting is treated as an annual event, these three time ratios correspond to a total

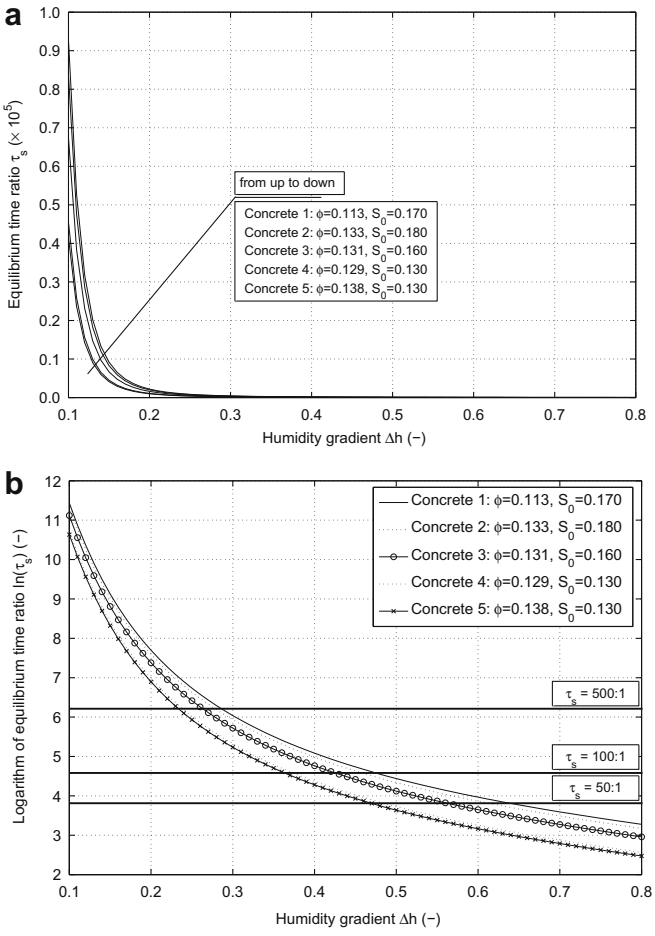

Fig. 2. Equilibrium time ratio τ_s in term of drying humidity gradient Δh for concrete sorption data from Hall [13]. (a) τ_s in normal magnitude and (b) τ_s in logarithm.

annual wetting time of 172, 87, and 17 h. It is observed that, for commonly encountered drying humidity gradient 30–40%, the time ratio τ_s is situated between 100 and 500, i.e. only 17–87 h are needed for a stabilized drying–wetting front while 87–172 h of wetting are necessary to stabilize the front for humidity gradient 40–50%.

4. Influential depth

4.1. Simple drying process

For a simple drying process, the drying front X_d at the end of drying can be evaluated from Eq. (7) as,

$$X_d = 2\lambda\sqrt{D_v t_d} = 2\lambda(T,\Delta h)\sqrt{D_v(T,\phi,s_l)t_d} \tag{21}$$

with D_v specified by Eqs. (17) and (18) and λ by the solution of Eq. (8). Fig. 3 illustrates the evolution of $X_d/\sqrt{t_d}$ in terms of concrete porosity ϕ and external drying gradient Δh for an ambient temperature T = 293 K. The Boltzmann variable $X_d/\sqrt{t_d}$ represents the drying front progression rate and it is observed that the progression is more rapid for larger porosity and higher humidity gradient.

4.2. Equilibrium influential depth

For a specific drying–wetting scheme, if the drying time t_d and wetting time t_w satisfy the equilibrium ratio, i.e. $t_d/t_w = \tau_s$, the stabilized drying–wetting front X_s can be evaluated by Eq. (7) as,

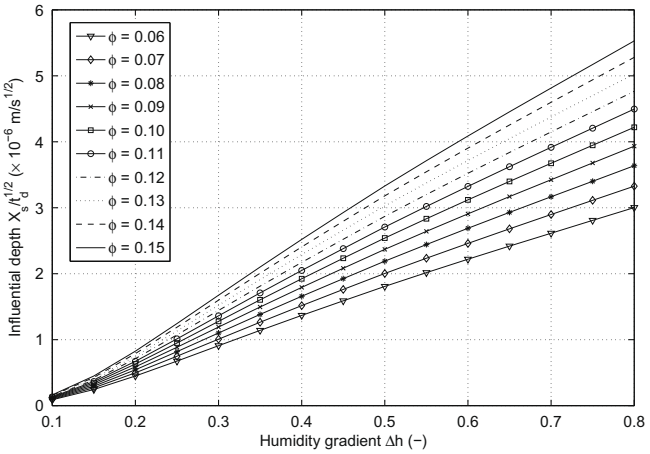

Fig. 3. Boltzmann variable $X_d/\sqrt{t_d}$ in terms of concrete porosity ϕ and drying humidity gradient Δh for ambient temperature T = 293 K.

$$X_s = 2\lambda\sqrt{D_v t_d} = 2\lambda\sqrt{D_v \tau_s t_w} \tag{22}$$

As aforementioned, if the drying–wetting is considered as an annual event, that is,

$$t_{event} = t_d + t_w = 1 \text{ year} \tag{23}$$

the influential depth X_s is thus,

$$X_s = 2\lambda\sqrt{D_v \frac{\tau_s}{\tau_s+1} t_{event}} \approx 2\lambda\sqrt{D_v t_{event}} \quad \text{with} \quad \tau_s \gg 1 \tag{24}$$

By this argument the stabilized front X_s can be evaluated independently from the equilibrium time ratio τ_s and in terms of its variables $T, \phi, \Delta h$ and s_l. The stabilized front X_s is calculated, for an ambient temperature of 293 K, in terms of porosity and humidity gradient, and the numerical results are presented in two dimensions and three dimensions, respectively, in Fig. 4a and b.

It can be seen that the influential depth of drying–wetting can be scaled to the order of 1 cm which is of the same magnitude of the concrete cover thickness for most concrete structural members exposed to natural drying–wetting. In durability design of reinforced concrete structures, assuring concrete cover with enough quality and thickness is crucial to the protection of internal steel reinforcement against corrosion. The numerical results obtained in the figures can serve as reference for the choice of concrete cover's quality, denoted by porosity ϕ, and its thickness, measured by the influential depth X_s. Qualitatively, one can state, from the figures, that for moderate drying gradient $\Delta h \sim 30\%$, the influential depth is within the first centimeter into concrete surface, for a gradient 30–50% this depth is situated within 1–2 cm and it can surpass 2 cm with a gradient higher than 50%. For comparison, most structural design codes specify a minimum concrete cover thickness more than 3 cm for drying–wetting environmental actions for durability consideration [19].

4.3. Influential depth evolution

Here come the more general cases: the time ratio of drying and wetting $\tau = t_d/t_w$ does not respect the equilibrium one τ_s. Hence, the drying–wetting front can not always be stabilized due to the unbalanced water loss and water intake. Two cases can be distinguished: $\tau > \tau_s$ and $\tau < \tau_s$.

For cycles $\tau > \tau_s$, more moisture is transported to outside during drying phase t_d than the water intake by absorption during wetting phase t_w, so it is a drying-dominated process. Consequently, each drying–wetting cycle contributes to the progression

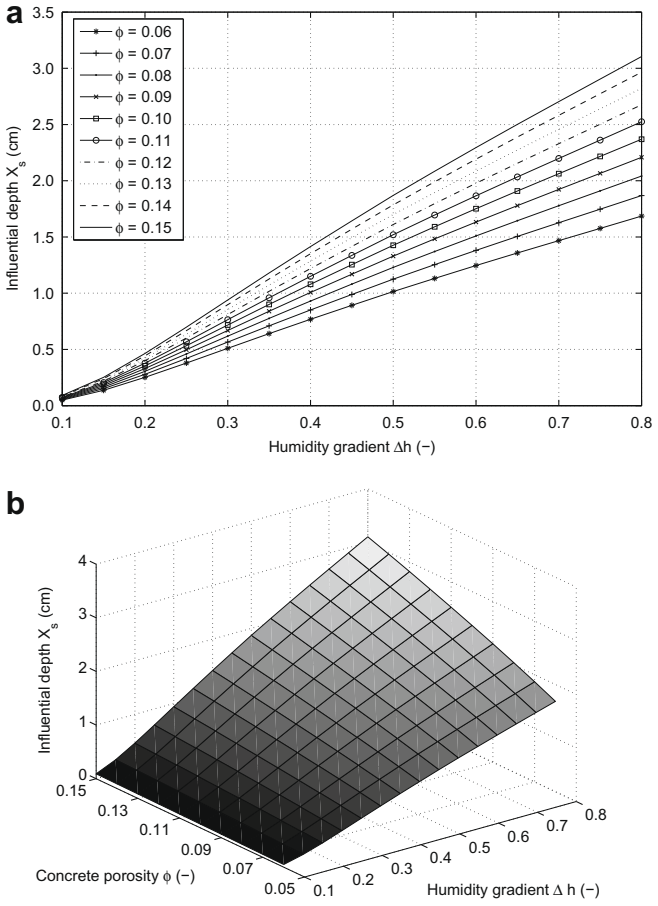

Fig. 4. Stabilized front X_s in terms of concrete porosity ϕ and drying humidity gradient Δh for ambient temperature $T = 293$ K. (a) Two dimensional illustration and (b) three dimensional illustration.

of drying front deeper into the material. At the end of each drying–wetting cycle, the difference between drying flow I_d and wetting flow I_w can be converted into the drying front progression dX,

$$\Delta I = 2\lambda\sqrt{D_v t_d}(s_s - s_0) - S_w\sqrt{t_w} = (s_s - s_0)dX \tag{25}$$

After n cycles the drying front, or influential depth, can be estimated as,

$$X_n = ndX = n\left(2\lambda\sqrt{D_v t_d} - \frac{S_w\sqrt{t_w}}{h_s - h_0}\right) \tag{26}$$

For a wetting-dominated process with $\tau < \tau_s$, more moisture flow can be absorbed during wetting than what is required to compensate the moisture loss during drying. Therefore, the drying front will disappear after each wetting phase. In other words, after each cycle the maximum influential depth of moisture transport is always determined by the drying time t_d,

$$X_n \equiv 2\lambda\sqrt{D_v t_d} \tag{27}$$

5. Conclusions

The models presented in the paper capture the main mechanisms involved in moisture transport across concrete surface subject to drying–wetting cycles. For the sake of developing an analytical approach, some details of moisture transport are neglected, such as the local elevation of water content near a drying front due to evaporation. Though simplified, these models do furnish several important conclusions concerning the drying–wetting front and its influential depth:

1. During the drying of an initially saturated concrete, the progression of the drying front is basically governed by three factors: external drying humidity, ambient temperature and vapor transport properties. From the numerical results, it can be observed that the front progression is sensitive, on one side, to material pore structure through total porosity ϕ and tortuosity resistance to vapor diffusion f; on the other side, front progression is sensitive to drying humidity gradient Δh through the coefficient λ. For a given climate condition, the dominating factor for drying front progression is the pore structure of concrete.
2. Under periodical drying–wetting cycles with drying time t_d and wetting time t_w, there exists an equilibrium time ratio $\tau_s = t_d/t_w$ by which moisture loss during drying is totally compensated by water intake by sorption during wetting. The drying front is thus stabilized and the corresponding influential depth at equilibrium can be evaluated. By this time ratio one can draw a first important conclusion if the moisture influential depth in concrete will evolve under a specific drying–wetting condition, which can be very helpful for the in situ analysis of moisture-related durability problems of structural concrete. From the numerical results, the influential depth at equilibrium can reach the magnitude of centimeters which is of the same order of concrete cover thickness in common design and construction practice.
3. For drying–wetting cycles with $t_d/t_w \neq \tau_s$, the paper gives quantitative expressions of influential depth evolution for drying-dominated and wetting-dominated processes. For drying-dominated process, one can employ the expression of influential depth evolution to predict moisture-related durability processes and furthermore to help the choice of strength class and thickness of concrete cover to steel reinforcement in structural members.
4. Although the modeling of influential depth is formulated on the basis of an initially water-saturated concrete, the same reasoning can be made for an initially dry material exposed to wetting and subsequent drying. Since the concepts of equilibrium time ratio and influential depth are formulated by the moisture flow balance between wetting and drying, the same expressions of influential depth and equilibrium time ratio can be applied for initially dry cases with the hypothesis that the head of wetting front after first wetting remains immobile during the subsequent drying.
5. The analytical modeling presented in this paper needs to be validated through comparisons with experimental results and the output of other models. The relevant issues can be found in other publications of the authors. For further engineering application of the analytical description of influential depth, however, the evaluation of wetting time t_w for natural climate conditions deserves some attention. According to the modeling, t_w is defined as the period during which the concrete surface is covered by a water film with sufficient thickness to mobilize concrete capillary sorption. Accordingly it can be different from, and usually much shorter than, the common definition of time-of-wetting (TOW) proposed for metallic surface corrosion processes.

Acknowledgement

The research is supported by National Natural Science Foundation of China (NSFC), Project No.50538060.

Appendix A. Solution of moving boundary problem

The goal is to solve the Stefan-like problem posed by Eqs. (3), (4) and (6). Introduce firstly an intermediate variable η,

$$\eta = \frac{x}{2\sqrt{D_v t}} \tag{28}$$

It is shown that the general solution can be written into the form [20],

$$h = A\,\mathrm{erf}(\eta) + B \tag{29}$$

with erf as the error function and A, B as constants. Consider the second boundary condition in Eq. (4),

$$h(\eta = 0) = h_0 \quad \Rightarrow \quad B = h_0,\ h - h_0 = A\,\mathrm{erf}(\eta) \tag{30}$$

Substitution of above equation into the first boundary condition in Eq. (4), one has

$$h_s - h_0 = A\,\mathrm{erf}\left(\frac{X}{2\sqrt{D_v t}}\right) \tag{31}$$

Here, we note

$$\lambda = \frac{X}{2\sqrt{D_v t}} \quad \text{and} \quad X = 2\lambda\sqrt{D_v t} \tag{32}$$

Introducing Eq. (32) into Eq. (31), one gets

$$A = \frac{h_s - h_0}{\mathrm{erf}(\lambda)} \tag{33}$$

and substitution of the above expression into Eq. (30) gives

$$h - h_0 = \frac{\mathrm{erf}(\eta)}{\mathrm{erf}(\lambda)}(h_s - h_0) \tag{34}$$

The solution of λ can be resorted to the moving boundary condition Eq. (6). The differential terms in the equation are,

$$\begin{cases} \frac{dX}{dt} = \lambda\sqrt{\frac{D_v}{t}} \\ \frac{\partial h}{\partial x} = \left[\frac{h_s - h_0}{\mathrm{erf}(\lambda)}\right]\mathrm{erf}'(\lambda)\frac{1}{2\sqrt{D_v t}} \end{cases} \tag{35}$$

So Eq. (6) becomes

$$\rho_l \lambda = \frac{1}{2} p_{vs}\frac{M_v}{RT}\left[\frac{h_s - h_0}{\mathrm{erf}(\lambda)}\right]\mathrm{erf}'(\lambda) \tag{36}$$

Note,

$$\mathrm{erf}(\lambda) = \frac{2}{\sqrt{\pi}}\int_0^{\lambda} \exp(-y^2)dy \quad \text{and} \quad \mathrm{erf}'(\lambda) = \frac{2}{\sqrt{\pi}}\exp(-\lambda^2) \tag{37}$$

Putting these results into Eq. (36), one gets

$$\rho_l \lambda = \frac{1}{\sqrt{\pi}} p_{vs}\frac{M_v}{RT}\left[\frac{h_s - h_0}{\mathrm{erf}(\lambda)}\right]\exp(-\lambda^2) \tag{38}$$

Rearranging the above equation gives the one variable equation for λ in Eq. (8). With solved λ the humidity profile can be calculated by Eq. (34) and the drying front X by Eq. (32).

References

[1] Bijen J. Durability of concrete structures: design, repair and maintenance. Cambridge: Woodhead Publishing; 2003.
[2] Hobbs DW, Matthews JD, Marsh BK. Minimum requirements of durable concrete: carbonation- and chloride-induced corrosion, freeze-thaw attack and chemical attack. Crowthorne: British Cement Association; 1998.
[3] DuraCrete. Probabilistic performance based durability design of concrete structures: modelling of degradation. DuraCrete Project Document BE95-1347/R4-5. The Netherlands; 1998.
[4] Cerny R, Rovnanikova P. Transport process in concrete. London: Taylor & Francis; 2002.
[5] McCarter WJ, Watson DW, Chrisp TM. Surface zone concrete: drying, absorption and moisture distribution. ASCE J Mater Civ Eng 2001;13(1):49–57.
[6] Nilsson LO, Poulsen E, Sandberg P, Sorensen HE, Klinghoffer O. Chloride penetration into concrete, state-of-art, transport process corrosion initiation, test method and prediction methods. HETEK Report No.53. Kobenhavn: The Danish Road Directorate; 1996.
[7] DuraCrete. Probabilistic performance based durability design of concrete structures: models for environmental actions on concrete structures. DuraCrete Project Document BE95-1347/R3. The Netherlands; 1998.
[8] Arfvidsson J. A new algorithm to calculate the isothermal moisture penetration for periodically varying relative humidity at the boundary. Nord J Build Phys 1999;2. <http://www.byv.kth.se/avd/byte/bphys>.
[9] Cunningham MJ. Effective penetration depth and effective resistance in moisture transfer. Build Environ 1992;27(3):379–86.
[10] Cunningham MJ. Moisture diffusion due to periodic moisture and temperature boundary conditions – an approximate steady analytical solution with non-constant diffusion coefficients. Build Environ 1992;27(3):367–77.
[11] Martys NS, Ferraris CF. Capillary transport in mortars and concrete. Cement Concrete Res 1997;27(5):747–60.
[12] Neithalath N. Analysis of moisture transport in mortars and concrete using sorption–diffusion approach. ACI Mater J 2006;103(3):209–17.
[13] Hall C. Water sorptivity of mortars and concretes: a review. Mag Concrete Res 1989;41(147):51–61.
[14] Bernardiner MG. A capillary microstructure of the wetting front. Transport Porous Med 1998;30:251–65.
[15] Mainguy M. Modeling of moisture transfer isotherms of porous media. Application to the drying of cement-based materials. Ph.D thesis. Ecole Nationale des Ponts et Chaussées, Paris, France; 1999 [in French].
[16] de Vries DA, Kruger AJ. On the value of the diffusion coefficient of water vapor in air. In: CNRS, editor. Phénomènes de transport avec changement de phase dans les milieux poreux ou collo, Proceedings of international colloquium CNRS, vol. 160; 1966. p. 61–72.
[17] Philip JR, de Vries DA. Moisture movement in porous materials under temperature gradients. Transac Am Geophys Un 1957;38(2):222–32.
[18] Baroghel-Bouny V. Water vapour sorption experiments on hardened cementitious materials, part I: essential tool for analysis of hygral behaviour and its relation to pore structure. Cement Concrete Res 2007;37(3):414–37.
[19] European Committee for Standardization. Eurocode 2: Design of concrete structures – part 1: general rules and rules for buildings (European standard prEN1992-1-1). CEN, Brussels; 2002.
[20] Gebhart B. Heat conduction and mass diffusion. New York: McGraw-Hill; 1993.